Power System Resilience to Extreme Weather: Fragility Modeling, Probabilistic Impact Assessment, and Adaptation Measures

Mathaios Panteli, *Member, IEEE*, Cassandra Pickering, Sean Wilkinson, Richard Dawson, and Pierluigi Mancarella, *Senior Member, IEEE*

***Abstract*—Historical electrical disturbances highlight the impact of extreme weather on power system resilience. Even though the occurrence of such events is rare, the severity of their potential impact calls for 1) developing suitable resilience assessment techniques to capture their impacts and 2) assessing relevant strategies to mitigate them. This paper aims to provide fundamentals insights on the modeling and quantification of power systems resilience. Specifically, a *fragility model* of individual components and then of the whole transmission system is built for mapping the real-time impact of severe weather, with focus on wind events, on their failure probabilities. A probabilistic multitemporal and multiregional resilience assessment methodology, based on optimal power flow and sequential Monte Carlo simulation, is then introduced, allowing the assessment of the spatiotemporal impact of a windstorm moving across a transmission network. Different risk-based resilience enhancement (or adaptation) measures are evaluated, which are driven by the *resilience achievement worth* index of the individual transmission components. The methodology is demonstrated using a test version of the Great Britain's system. As key outputs, the results demonstrate how, by using a mix of *infrastructure* and *operational* indices, it is possible to effectively quantify system resilience to extreme weather, identify and prioritize critical network sections, whose criticality depends on the weather intensity, and assess the technical benefits of different adaptation measures to enhance resilience.**

***Index Terms*—Critical infrastructure, extreme weather, fragility curve, resilience, resiliency.**

I. Introduction

EXTREME weather conditions, as high-impact low-probability (HILP) events, may affect significantly the operational resilience of a power system. Climate change projections indicate that the frequency and severity of such events might increase in the near future [1]. Therefore, power systems need to be not only reliable to the known and credible threats, but also resilient to HILP events.

The effect of severe weather, such as floods, hurricanes and ice storms, is increasingly evident on power networks worldwide [2]. Modelling the impacts of extreme weather on the reliability of power systems has mainly focused on characterizing the effect of weather conditions on the reliability attributes of power system components, i.e., failure and restoration rates. Different techniques have been used, such as Markov modelling (e.g. [3], [4]) and Sequential Monte Carlo simulation (SMCS) [5]–[8]. An extensive review of weather-related reliability assessment techniques is provided in [9], while methodologies and challenges of assessing the risk of cascading outages are provided in [10]. On the other hand, differently from the previous works more focused on reliability, resilience-oriented quantitative models, metrics and enhancement strategies have been developed in [11]–[18]. In this respect, an overview of previous research studies on resilience of power systems under natural disasters is presented in [19], and a framework for understanding, conceptualizing and boosting power systems resilience has been presented in [20] and [21]. However, these previous works (including [8] and [18] by the authors) do not describe how to build the *network fragility* model, or implement the comprehensive approach needed to quantify network resilience to extreme weather; likewise, it is not shown before how, by using a mix of *infrastructure* and *operational* indices, it is possible to demonstrate the benefits and implications of different enhancement strategies that target parts of the system specifically identified through a suitable algorithm.

On the above premises, this paper presents a comprehensive methodology for multi-temporal and multi-regional resilience assessment and enhancement of transmission systems to extreme weather conditions, with application on the impact modelling of severe windstorms on transmission networks. The approach is an extension of a CAT modelling approach used by the insurance industry to obtain the expected losses to an insurance portfolio for a given hazard (e.g. earthquake, flooding, wind etc.). This method is gaining popularity and has recently been adopted by the Federal Emergency Management Agency (FEMA) for their standardized method for estimating losses for

Manuscript received April 27, 2016; revised August 23, 2016 and November 9, 2016; accepted December 11, 2016. Date of publication December 29, 2016; date of current version August 17, 2017. This work was supported in part by the UK Engineering and Physical Sciences Research Council through the 'Resilient Electricity Networks for Great Britain' project under Grants EP/I035781/1 and EP/I035757/1) and in part by the UK-Chile 'Disaster management and resilience in electric power systems' project under Grant EP/N034899/1. Paper no. TPWRS-00654-2016.

M. Panteli is with The University of Manchester, Manchester M13 9PL, U.K. (e-mail: panteli.mat@gmail.com).

C. Pickering, S. Wilkinson, and R. Dawson are with Newcastle University, Newcastle NE1 7RU, U.K. (e-mail: c.pickering@ncl.ac.uk; sean.wilkinson@ncl.ac.uk; richard.dawson@ncl.ac.uk).

P. Mancarella is with The University of Manchester, Manchester M13 9PL, U.K., and also with The University of Melbourne, Parkville, Vic 3010, Australia (e-mail: p.mancarella@manchester.ac.uk).

Color versions of one or more of the figures in this paper are available online at http://ieeexplore.ieee.org.

Digital Object Identifier 10.1109/TPWRS.2016.2641463

earthquake, flood and hurricane (HAZUS) [22]. In this work, we extend this method to capture system impacts on electricity infrastructure due to severe windstorms. However, we argue that, as this simulation model and our resilience indices would be the same for other hazards, it is also applicable to these; nevertheless, a new hazard model and fragility curves would need to be used. It can also be argued that it is possible to apply the approach to hazards in combination; nevertheless, if the hazards are not independent then joint probability hazard models need to be developed. Similarly, if the infrastructure response is also dependent on two hazards (e.g. damage due to wind and ice) then fragility curves that consider the combination of these hazards being experienced must be used. In our modelling framework, a time-series probabilistic simulation model is presented, which stochastically models and evaluates the spatiotemporal impact of weather fronts as they move across a large-scale transmission network. A fragility model of power system components is developed and thoroughly presented in this paper to characterize their failure probability as a function of the weather they experience at any given time.

The time- and spatial-dependent reliability features of all components are then fed into a SMCS engine to estimate, supported by Optimal Power Flow (OPF), specific reliability indices that are used to capture the *operational* effect of the weather event. Different from previous works (including work by the authors), these are used in combination with other *infrastructure* indices (e.g., number of lines going offline) in a risk-based fashion to quantify the impacts of a windstorm and the degradation in the resilience of a power system, as well as support the development of resilience enhancement strategies.

For the latter, the Cabinet Office, UK [23] identifies resistance, redundancy and response/recovery as key resilience features. Therefore, here we evaluate different resilience enhancement strategies that are well in line with these key resilience features, namely, making specific corridors more *robust/resistant* or *redundant*, or making the repairing crews more *responsive*. Following the approach proposed in [24], the criticality of individual components within a system and where to apply these resilience measures are selected based on an algorithm that estimates the *Resilience Achievement Worth* (*RAW*) index of individual corridors. This is performed for different windstorm intensities, allowing the evaluation of the criticality of each corridor and the effectiveness of these strategies under varying stress imposed by the windstorm.

Summarizing, the key contributions of this work are:

1) the development of structural fragility curves for transmission elements by civil engineers and their effective integration into an advanced power system model in collaboration with electrical power engineers, thus effectively developing a *system resilience* model that accounts for both infrastructure and operational aspects;
2) a SMCS-based simulation engine for assessing the *time-varying* and *space-varying* impact of extreme weather on power systems resilience using fragility curves and multi-temporal optimal power flow;
3) a specifically introduced mix of operational and infrastructure indices, based on consolidated and thus simple to interpret reliability indices, aimed at getting a more complete picture of the resilience degradation due to the extreme event for increasing intensities (i.e., increasing maximum wind speeds);
4) a general technique for the identification of resilience-critical components and the prioritization of relevant, specific interventions;
5) the demonstration that this criticality is dependent on the weather intensity and hence that the adaptation planning and reinforcement strategies need to be flexible; and
6) the impact evaluation of different resilience enhancement strategies in line with key resilience features.

The rest of the paper is organized as follows. Section II presents the fragility modelling and resilience assessment of transmission corridors, while Section III discusses transmission network probabilistic resilience assessment and enhancement procedure. The designed models are illustrated in Section IV using a reduced version of the GB transmission network. Section V summarizes and concludes the paper.

II. Fragility Modelling and Resilience Assessment of Transmission Components and Corridors

A system model has been developed to assess the impact of windstorms on the resilience of transmission networks. This includes the fragility modelling of individual towers and lines and the assessment of resilience to severe windstorms.

A. Modelling Assumptions

National scale risk analysis of complex, coupled environmental-engineering systems presents particular challenges in terms of data acquisition, numerical computation and presentation of results. Therefore, a methodology has been developed here that addresses these difficulties through the following appropriate approximations that reduce the complexity of the processes being considered whilst capturing key system behavior, but without affecting the generality and applicability of the methodology itself:

1) Generation is not directly affected by the windstorm (with the exception of wind generation), although generation nodes can be disconnected due to outages of transmission corridors.
2) Load does not change before, during and after the weather event; it is thus considered weather-independent.
3) All towers and lines in the test system used are assumed to share the same fragility function. Tower fragility is derived from structural analysis modelling, whereas line fragility is based on a statistical analysis [25].
4) Whilst towers are designed to common standards, there are some variations in design (e.g., terminal and angle towers) and although towers are fully refurbished every 20 years, the precise condition of each tower is not known.
5) The outage of each transmission tower is considered to be independent of the condition of adjacent towers.

6) Due to lack of actual restoration times of the collapsed/damaged transmission corridors following extreme weather, times to repair are based on expert judgement (in discussion with the system operator) and limited reported data from international studies [26], but adjusted to reflect the increasing damage and time to repair for higher wind speeds.
7) Due to lack of the wind conditions experienced by the transmission corridors with the desired spatial and temporal resolution, the test network in the case study application is divided into regions which are assumed to have homogenous weather conditions.
8) AC OPF is used as a dispatch tool.

B. Tower Fragility Modelling

A *fragility function* describes the probability of failure of a structure or structural component, conditional on a loading that relates the potential intensity of a hazard (e.g., wind speed on a transmission tower) and as such, it is useful for inclusion in Monte-Carlo based risk assessments of populations of infrastructure assets to a given hazard [27], [28].

Fragility curves can be derived: (i) empirically from statistical analysis of a large set of observed failures, (ii) experimentally by deliberately failing towers, (iii) analytically using a structural simulation model, (iv) using expert judgment, or (v) through a combination of these methods. Empirical curves can often be constructed for distribution network towers for which there are more failure records due to their greater number and lower design standard [29]. However, in the case here *analytical* fragility curves had to be produced as there are insufficient wind-related failures of transmission towers in the UK and globally to develop empirical curves. Also, towers are generally too large and expensive to destroy to consider a full scale experimental program, effectively ruling out (ii). Finally, expert judgement would be highly uncertain as there might be too few experiences to draw on.

A broad-scale system analysis requires a fragility function that captures the structural performance and associated uncertainties (e.g., due to different deterioration rates) of a population of similar assets. These only need to be described to a precision commensurate with the other aspects of the system analysis. The methodology used here has been adapted by transferring the principles set out by the Applied Technology Council (ATC 58), which was developed for the Federal Emergency Management Agency to improve the structural performance of buildings to seismic hazards [30], to calculate failure probabilities of power system components as a function of wind loading.

Many structural engineering phenomena, such as material strength properties in laboratory specimens, have a lognormal distribution. For a given hazard intensity (e.g., wind speed associated with a particular threshold of structural damage), the probability of being in, or exceeding, a damage state *ds* is described by the lognormal function:

$$P\left[ds|S_d\right] = \Phi\left[\frac{1}{\beta_{ds}} \ln\left(\frac{S_d}{\bar{S}_{d,ds}}\right)\right] \tag{1}$$

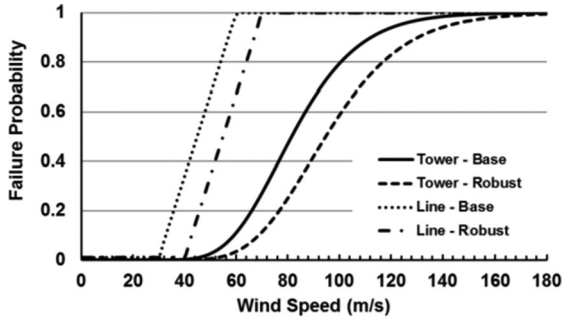

Fig. 1. Wind fragility curves of transmission lines and towers (base and robust case studies).

where: $\bar{S}_{d,ds}$ is the median value of engineering demand parameter (e.g., displacement or stress) at which the asset reaches the threshold of the damage state *ds*; β_{ds}, is the standard deviation of the natural logarithm of engineering demand parameter at which the asset reaches the threshold of the damage state *ds*; and Φ is the standard normal cumulative distribution function.

A structural model of the UK National Grid L2 transmission towers was analyzed using the commercially available ABAQUS software. Beam finite elements were used to represent structural members. Forces on the structure were calculated using European codes and the UK national annexes: self-weight of insulators and conductors were obtained from BS EN 50341-1 and wind loads were calculated using BS EN50341-1, which is broadly consistent with other approaches (e.g., [31]). Analysis of both geometrical and material nonlinearities, under a range of wind loadings, was used to construct the tower fragility curve, shown in Fig. 1 ("base" case), and expressed as:

$$P_T(w) = \begin{cases} 0, & \text{if } w < w_{\text{critical}} \\ P_{T\_hw}(w), & \text{if } w_{\text{critical}} \le w < w_{\text{collapse}} \\ 1, & \text{if } w \ge w_{\text{collapse}} \end{cases} \tag{2}$$

where $P_T(w)$ describes tower failure probability as a function of wind speed (*w)*, *hw* stands for high winds, w_{critical} is the wind speed at which the tower's failure probability picks up and w_{collapse} is the wind speed at which the tower has a negligible probability of survival (considered to be 45 m/s and 150 m/s here, respectively). When connected in series, collapse of a single tower trips the transmission corridor:

$$\begin{aligned} &P[\text{Towers Failure}] = 1 - P[\text{Towers Survival}] \\ &= 1 - P[(F_1 = 0) \cap (F_2 = 0) \cap ..... \cap (F_N = 0)] \end{aligned} \tag{3}$$

where *F* is the failure function of an individual tower and *N* is the number of towers across the transmission corridor, which is given by the ratio of the corridors' length and the distance between the towers (taken as between 300 m and no more than 400 m depending on overall corridor length). Although failure of one tower can lead to increased mechanical forces on adjacent towers, no such instance has been recorded in Great Britain, and modeling studies and empirical data from North America suggest that this is extremely uncommon for wind loading of

high voltage lattice transmission towers [32], [33]. In keeping with the principles of system analysis, transmission towers are therefore assumed to fail independently of one another, so that (3) can be simplified as:

$$P[\text{Towers Failure}] = 1 - \prod_{k=1}^{N} (1 - P_k) \tag{4}$$

which is further simplified if the tower failure probabilities are assumed to be the same for each tower:

$$P[\text{Towers Failure}] = 1 - (1 - P_T(w))^N \tag{5}$$

where $P_T(w)$ is the individual tower failure probability as obtained by (2). If the wind conditions experienced by a transmission tower are accurately available with appropriate spatial and temporal resolutions, they can be used to define the exact, individual wind-dependent failure probability of each tower across a transmission corridor.

C. Line Fragility Modelling

The resilience of a transmission line is similarly affected by local weather conditions, which may result in the failure of the line due to several reasons, e.g., shackle failure. The failure of a line is considered to be independent from pylon failure, so a different weather fragility curve is needed.

An example of a line fragility curve is depicted in Fig. 1 ("base" case), which relates the failure probability of a transmission line to the wind speed. Similarly to (2):

$$P_L(w) = \begin{cases} \overline{P_L}, & \text{if } w < w_{\text{critical}} \\ P_{L\_hw}(w), & \text{if } w_{\text{critical}} \le w < w_{\text{collapse}} \\ 1, & \text{if } w \ge w_{\text{collapse}} \end{cases} \tag{6}$$

where $P_L(w)$ refers to the line failure probability as a function to the wind speed. $\bar{P}_L$ is the "good weather conditions" failure rate, considered equal to 1×10^{-2} here. A linear relation between the lines' failure probability and high wind speeds between w_{critical} and w_{collapse} is applied, which are considered equal to 30 m/s and 60 m/s respectively. The w_{critical} used here is in line with a statistical study performed in [25], which relates the lines' failure probability in GB to wind speed. Empirical statistical data from the electrical utility can be used to adjust these fragility curves to reflect the real behavior of the lines.

D. Transmission Corridor Resilience Assessment

Fig. 2 shows the generic simulation procedure for determining the effect of any hazard on the status of each transmission corridor at every simulation step of the SMCS approach. In this specific application, the hazard *h* refers to the windstorm intensity (*w*). Hence, the $P_L(h)$ and $P_T(h)$ in Fig. 2 correspond to $P_L(w)$ and $P_T(w)$ respectively.

At simulation step *i*, the wind intensity (w_i) is calculated and integrated over the wind fragility curves of Fig. 1, which provides $P_T(w_i)$ and $P_L(w_i)$. A corridor outage can occur due to a conductor failure or a tower collapse. The latter can cause a double circuit failure if the two circuits are on the same tower, which is a Common Cause Failure (CCF).

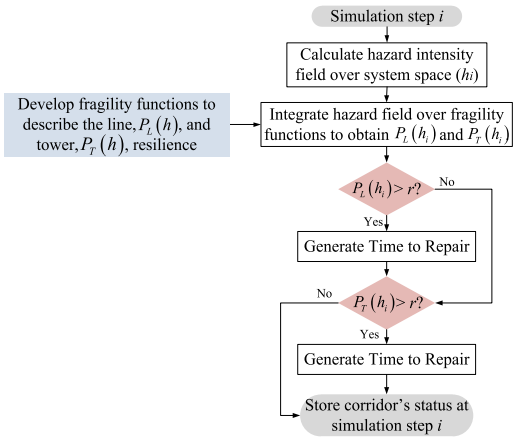

Fig. 2. Generic component approach for determining the effect of a hazard on the status of a transmission corridor at every simulation step.

After obtaining the wind-dependent failure probability of the transmission corridor (i.e., $P_L(w_i)$ and $P_T(w_i)$), it is evaluated if the corridor will trip at this simulation step by comparing $P_L(w_i)$ and $P_T(w_i)$ with a uniformly distributed random number $r \sim U(0,1)$. As these failure probabilities of the transmission components are dynamically updated every step of the SMCS procedure depending on the prevailing weather conditions, the random number *r* is generated and compared with the failure probabilities each hour. A single circuit outage occurs if:

$$F_L(w_i, L_i) = \begin{cases} 0, & \text{if } P_L(w_i) < r \\ 1, & \text{if } P_L(w_i) > r \end{cases} \tag{7}$$

where F_L is the failure function of the transmission line, while a double-circuit outage due to a tower collapse occurs if:

$$F_T(w_i) = \begin{cases} 0, & \text{if } P_T(w_i) < r \\ 1, & \text{if } P_T(w_i) > r \end{cases} \tag{8}$$

where F_T is the failure function of the transmission tower. It has to be noted here that $P_L(w_i)$ and $P_T(w_i)$ are compared independently with *r* because the effect of $P_L(w_i) > r$ (i.e., line outage) and $P_T(w_i) > r$ (i.e., tower outage) is different, i.e., a single and double circuit outage respectively.

Following a line or tower outage, the Time to Repair (*TTR*) is randomly generated. The *TTR* represents the time required for repairing a fallen line or tower, i.e., the time required for the repair crew to get to the affected areas, transfer the spare components and restore to service the tripped components. A different *TTR* for the transmission lines and towers is required. The *TTR* of these components under normal weather (TTR_{normal}) can increase at higher wind speeds due to increased overall damage as well as subsequent accessibility of the affected areas. In particular, three damage levels are considered here: low, moderate and severe. To reflect the increasing corridor damage, a *TTR* that increases with the damage level is used, which helps capture an additional dimension of resilience: the effect of extreme weather events on the restoration time of faulted components. The damage level is determined here based on the maximum wind speed ($w_{\max}$) of the wind profile that would cause the highest

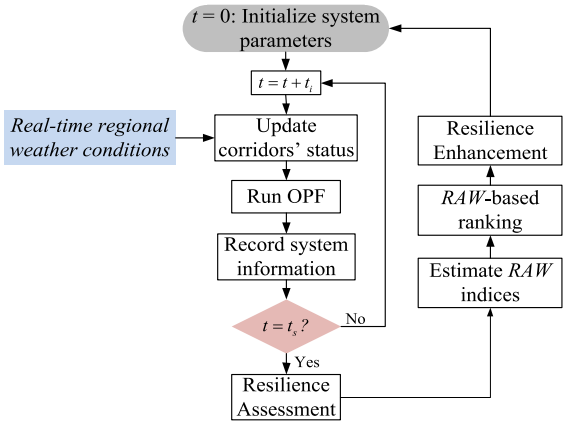

Fig. 3. System approach for resilience assessment and enhancement.

damage to the corridors. A uniformly distributed random factor within a predetermined range is then used to multiply TTR_{normal} for each damage level.

By applying the procedure set out in Fig. 2 to every transmission corridor, their wind-affected operational state, including power flows evaluated using an OPF engine, at every simulation step of the SMCS procedure can be obtained. This is critical in modelling the behavior of the transmission corridors under the real-time operating conditions they experience. The continuous update of the corridors' status based on the prevailing weather conditions using the fragility curves allows the realistic modelling of the weather event as a continuously fluctuating phenomenon.

III. Transmission System Probabilistic Resilience Assessment and Enhancement

This Section describes the probabilistic resilience assessment approach for the whole system considering moving weather fronts, and then introduces the *RAW* index based on which resilience enhancement strategies can be carried out.

A. Multi-Temporal and Multi-Regional Resilience Assessment

Fig. 3 shows the simulation procedure for assessing system resilience to real-time operating conditions (indicated by the inner loop). After initializing the system parameters at $t = 0$, the approach of Fig. 2 is followed for updating the corridors' status at each simulation step based on the prevailing real-time operating and weather conditions.

In the majority of the weather-related studies in the distribution networks, it is usually considered that the entire network is exposed to the same weather conditions. However, in transmission networks, the impact of a weather event varies as the weather front moves across the network. In this study, in order to account for the spatial weather impact in different transmission areas, the transmission network is arbitarily divided into six regions which are assumed to have homogeneous weather conditions. If the wind profiles with the desired spatial resolution and accuracy along the transmission corridors were available, then they could be used in the simulations instead of dividing the network in regions.

The weather-dependent failure probabilities are then fed to the AC OPF-based SMCS to capture the multi- temporal and multi-regional impact of these real-time operating conditions. It has to be noted here that even though AC OPF is considered an appropriate dispatch tool for this specific application, it does not consider other important relevant issues, such as transient stability and unit commitment. However, the proposed tool offers the capability and flexibility to include such constraints for modelling additional dimensions of the problem. The weather model is calibrated against hourly time steps and so this is used as the simulation step (t_i) here. Nevertheless, even higher time resolution could be used in this approach, if the relevant data were available. The OPF is run at each step and until the end of the simulation (t_s) is reached. For the purposes of the OPF implementation, the load shedding that might occur at each simulation step is considered equal to the output of very expensive, virtual generators placed at the load buses of the network.

At the end of the simulation period t_s, the multi-temporal and multi-regional system resilience is assessed and evaluated. For this purpose, in this paper specific reliability indices (i.e., Loss of Load Frequency (*LOLF*, occs/year) and Expected Energy Not Supplied (*EENS*, MWh/year)) and the generation capacity going offline during the weather event are used to reflect the *operational* effect of the weather event, supported by *infrastructure* indices, and in particular the number of transmission lines going offline due to extreme weather. The use of both *operational* and *infrastructure* indices allows the systematic risk-based assessment of the resilience degradation of a power system subject to severe weather. This also enables the evaluation of the benefits of options considered important for critical infrastructures by Cabinet Office, UK [23].

B. Resilience Enhancement Analysis and Adaptation Measures

The aim of this study is to provide insights into potential strategies to enhance network resilience against future (similar or unforeseen) events. A number of resilience enhancement strategies may be considered for adaptation, especially if the resilience level resulting from specific studies is deemed insufficient. Therefore, following the resilience assessment, different options for boosting the key features of power grid resilience are evaluated as shown in Fig. 3. In this work the impact of the following enhancement options are considered:

a) *Redundancy,* by adding identical transmission lines in parallel with the existing ones;
b) *Robustness,* improving the resistance of the components to the weather event (as shown in Fig. 1, i.e., shifting the fragility curves of the transmission lines and towers to the right, making them more robust to high wind speeds); and
c) *Responsiveness,* whereby it is assumed the weather event has no impact on *TTR*, i.e., no multiplication factor is used for increasing TTR_{normal} for high wind speeds.

Strategies (a) and (b) aim to boost the infrastructure resilience of the network, while strategy (c) aims to improve its operational resilience and reaction to the weather event.

In order to apply targeted, risk-based resilience enhancement actions, information is required on the criticality and contribution of each transmission corridor to the overall network resilience. For this purpose, the index *RAW* [24] is used here, which here expresses the percentage improvement in the resilience indices when each line is considered 100% reliable during the simulations:

$$RAW = \frac{R_s - R_s(R_n = 1)}{R_s} \times 100 \tag{9}$$

where R_s = system resilience index (e.g., *EENS*), R_n = individual corridor's reliability and $R_s(R_n = 1)$ shows the system resilience by considering that corridor n will never fail during the simulation procedure (i.e., $R_n = 1$). Therefore, $R_s - R_s(R_n = 1) > 0$. Then, the *RAW* indices of the transmission corridors are ranked to determine the most critical corridors and suitable adaptation strategies can be in case assessed (see Fig. 3). It has to be clarified that the estimation of the *RAW* indices and the criticality ranking of the transmission corridors refer only to the time period when the network is subject to the extreme weather and for the purposes of resilience assessment only.

IV. Case Study Application to Great Britain Reduced Transmission Network

This section presents the illustration of the proposed probabilistic resilience assessment tool, with application on the impact modelling of severe windstorms (as HILP event) on a reduced version of the GB transmission network. A simulation period of one winter week is used (i.e., $t_s = 168$ hrs), where the peak demand and extreme winds in GB are expected.

A. Test Network and Regional Wind Profiles

The proposed approach is illustrated using a reduced 29-bus version of the GB transmission network (Fig. 4). This model consists of 29 nodes, 98 overhead transmission lines in double circuit configuration (which are assumed to be on the same tower) and one single circuit transmission line (i.e., between nodes 2 and 3) and 65 generators with an installed capacity of 75.3 GW, which are located at 24 nodes and include several generation technologies such as wind, nuclear, CCGT etc. This GB reduced network is based on and has been validated against a solved AC Load Flow reference case that was provided by National Grid Electricity Transmission (NGET), the transmission system operator of GB [34] and it shows the main transmission routes.

Without losss of generality, the test network is arbitrarily divided into 6 weather regions (Fig. 4(b)) to model the spatial and regional impact of the wind event as discussed earlier. Data permitting more regions could be used. In this way, the wind event can travel at any direction across the network. As can be seen in Fig. 4(b), some transmisison corridors cross two weather regions (e.g., line 1-2), experiencing different wind conditions

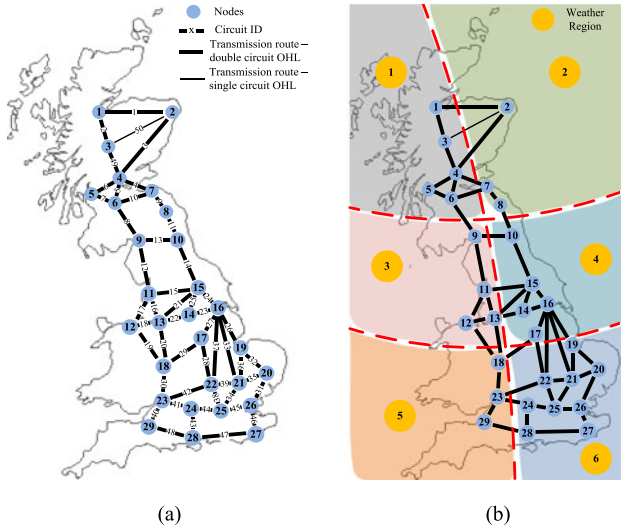

Fig. 4. The reduced 29-bus Great Britain transmission network. a) Transmission network. b) Weather regions.

in each region and in turn different wind failure probabilities. In this case, the worst weather conditions that the corridor is experiencing among these weather regions is considered for obtaining its weather-dependent failure probability and modelling its *TTR*.

The time-series regional wind profiles are obtained using MERRA re-analysis [35]. Time-series wind profiles for 33 years with an hourly time resolution are generated, and then a winter week, hourly wind profile is randomly selected among the 33 years for each SMCS trial. These wind profiles were generated at different locations within each region, and then the wind profile with the maximum wind speeds (that would cause the largest damage to the transmission corridor) was chosen as representative for each region in order to model the "worst-case" windstorm scenarios that could hit the network.

According to the UK MET office [36], the highest low-level wind speed ever recorded is approximately 63.5 m/s. Such high values in the MERRA wind data are very rare. In order to obtain wind speeds that can threaten the resilience of the system, the hourly wind profiles obtained by MERRA re-analysis are scaled-up (i.e., using a multiplication factor for the entire wind profile) to generate hourly wind profiles with absolute maximum wind speeds close to the historical one. Fig. 5 shows the probability density function of the regional wind profiles with $w_{\max} =$ 40 m/s and Fig. 6 depicts an example of the hourly regional wind profiles with the same $w_{\max}$.

Following this approach, multiple hourly wind profiles with increasing absolute maximum wind speeds are obtained. The simulations are then carried out for each one of these hourly wind profiles, in order to determine the wind speeds at which the test network becomes less resilient.

It is worth noticing that, although extreme wind does have a predominant direction (240° from North for the UK), this has not been included in this study because the direction of extreme wind obtained from MERRA is not at ground level and will be affected by a number of factors (e.g., altitude, terrain and

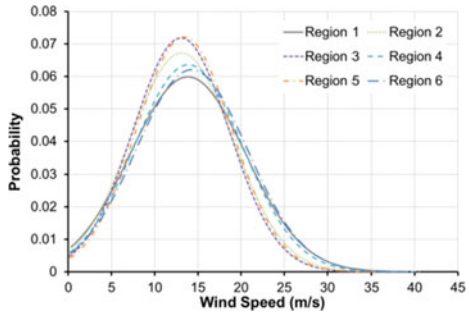

Fig. 5. Probability density function of regional wind profiles with $w_{\max} =$ 40 m/s.

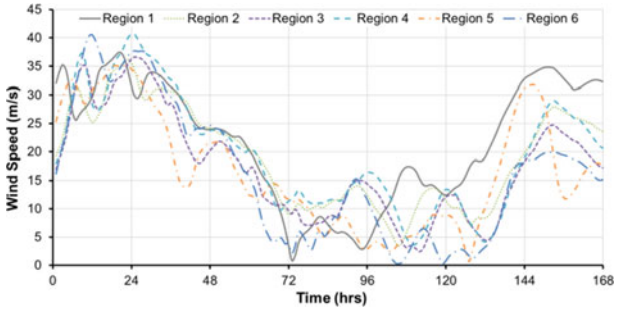

Fig. 6. An example of the hourly regional wind profiles with $w_{\max} = 40$ m/s.

orography) which may significantly change its angle of attack at the ground surface. Based on the resolution of existing reanalysis data sets (approximately 50 km over the UK), it is therefore not possible to correct for these influences as they occur on lower spatial scales than the reanalysis data. Furthermore, as there are no documented cases of a large number of wind related tower failures in the UK, it is then not possible to assess whether the method would be improved with the inclusion of direction.

In general, the repair times of the damaged transmission lines and towers would ideally be provided by the network operators, based on analysis of a large sample of experiences/historical databases and the emergency and restoration policies and procedures in place. In this case study application, assumptions were made following discussions with National Grid, the GB transmission system operator, which also provided feedback on the application. Specifically, the *TTR* is assumed to be 10 hours for the lines and 50 hours for the towers under normal weather conditions (i.e., TTR_{normal}), which also falls within the the range of case studies reported by [26]. The three damage levels are defined here as follows: $w_{\max} \leq 20$ m/s, $20 < w_{\max} \leq 40$ m/s and $40 < w_{\max} \leq 60$ m/s for low, moderate and severe damage levels respectively. Then, the *TTR* of the components under these damage levels is determined as:

$$TTR = \begin{cases} TTR_{\text{normal}}, & w_{\max} \leq 20 \text{ m/s} \\ k_1 \times TTR_{\text{normal}}, & 20 \text{ m/s} < w_{\max} \leq 40 \text{ m/s} \\ k_2 \times TTR_{\text{normal}}, & 40 \text{ m/s} < w_{\max} \leq 60 \text{ m/s} \end{cases} \quad (10)$$

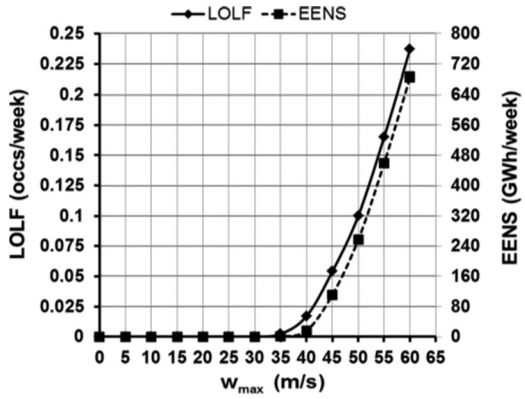

Fig. 7. Influence of wind on *LOLF* and *EENS* as a function of $w_{\max}$ of each wind profile for the base case.

where $k_1 \sim U(2,4)$ and $k_2 \sim U(5,7)$ are numbers randonly generated within these predetermined ranges. No multiplication factor is used for the low damage level. For example, if $w_{\max} =$ 15 m/s, then a *TTR* equal to TTR_{normal} is used. If $40 < w_{\max} \leq$ 60 m/s, then TTR_{normal} is multiplied by the random number k_2. In this case, it might take up to about two weeks to fully restore a highly damaged transmission tower. With no published information on these times, the range of k_1 and k_2, and the thresholds of $w_{\max}$, have been determined in consultation with the National Grid. In the *responsiveness* case study, it is assumed that $k_1 = k_2 = 0$.

B. Evaluating the Wind Impact on the Test Network

Fig. 7 shows the *operational* indices *LOLF* and *EENS* as a function of increasing $w_{\max}$ experienced for the base case study (i.e., no resilience measures applied). This study helps determine the threshold of the wind speeds at which the network becomes less operationally resilient, i.e., there is an increase in the frequency and severity of customer interruptions. The horizontal axis of Fig. 7 represents the maximum wind speed ($w_{\max}$) that the transmission corridors are imposed within the different wind profiles by adjusting the MERRA values.

It can be clearly seen that the test network is highly operationally robust to wind speeds below 30 m/s, as both *LOLF* and *EENS* are close to zero. For this range of wind speeds, which represents a severe storm based on the Beaufort wind force scale by Met Office, UK [37], the failure probabilities of the components are not affected by the wind event, as can be seen in the fragility curves of Figs. 1(a) and 1(b). The likelihood of cascading outages is thus low, resulting in low probability of customer disconnection. The operational resilience of the test system can effectively withstand a limited number of transmission outages, which prevents the failure propagation. However, for wind speeds higher than 30 m/s, which is the w_{critical} of the line wind fragility curves, a sharp, nonlinear increase in *LOLF* and *EENS* is observed. It is also worth noting that despite the low frequency of such events (as from the *LOLF*), the impact of windstorms with wind speeds higher than the threshold of 30 m/s can be significantly high, in line with the definition of HILP events.

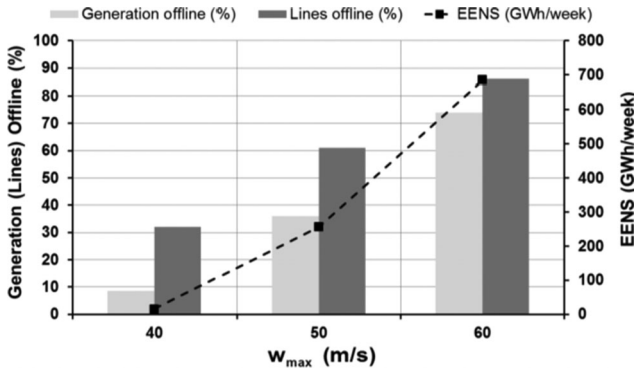

Fig. 8. Generation and transmission lines that went offline during windstorms with maximum wind speeds of 40, 50 and 60 m/s respectively.

Fig. 8 shows the percentage of transmission lines that went offline (i.e., *infrastructure indices*) during the windstorms with $w_{\max}$ of 40, 50 and 60 m/s, along with the percentage of the generation capacity not connected to the network due to transmission line outages and the corresponding *EENS* from Fig. 7 (i.e., *operational indices*). It can be seen that the infrastructure and operational indices perform very differently. For wind speeds up to 40 m/s the loss of transmission lines does not have a proportional loss of generation and demand; that is, owing to the available redundancy, the system can withstand the impacts of the windstorm, with nearly zero *EENS*. However, as the number of transmission line outages substantially grows under higher wind speeds resulting in a large degradation in the infrastructure resilience of the test network, the amount of generation loss and demand not served increases significantly, i.e., large decrease in the operational resilience. It is therefore possible to use *EENS* (or similarly *LOLF*) in conjunction with the infrastructure index (i.e., number of lines offline) to understand and quantify the impacts of the windstorm. Within this context, *EENS* will be used to support the targeted resilience enhancement strategies in the following sections.

C. RAW Results

The next step is to estimate the *RAW* indices of each transmission corridor using (9). This analysis is performed for three of the wind profiles used in the simulations, namely, the ones with maximum wind speeds equal to 40 m/s, 50 m/s and 60 m/s, respectively. This is done to evaluate the criticality of each circuit under different wind conditions. These *RAW* indices thus reflect the criticality of each circuit as related to the degree of how hard they are hit by the windstorms and to their contribution to not supplying the demand.

Fig. 9 shows the results of this study. In Fig. 9(a), the vertical axis represents the RAW_{EENS} (i.e., percentage decrease in *EENS* achieved by considering the transmission circuit 100% reliable), while the horizontal axis shows the circuits ranking (i.e., 1 to 50, the number of circuits of the test system) based on their RAW_{EENS} indices. For each ranking, the critical circuits for each wind level are provided (the circuit IDs are presented at the top of Fig. 9(a) and in Fig. 4(a)). Fig. 9(b) maps the RAW_{EENS} results on the test network for $w_{\max} = 40$ m/s.

It can be seen that the criticality of the lines changes between the wind profiles, as a different reduction in *EENS* is achieved. For example, circuit 45 is the most critical for all the wind levels, but the criticality of circuit 34 is ranked 2nd for $w_{\max} = 40$ m/s and 50 m/s, but 4th for $w_{\max} = 60$ m/s. This observation is key, because it supports potential investment decision on specific lines depending on the resilience goals. For example, if it is desired to boost the resilience to the extreme wind events, despite their much lower probability of occurrence, then the robustness of the lines with the highest RAW_{EENS} values for $w_{\max} = 50$ m/s or $w_{\max} = 60$ m/s (which can be considered as HILP events) has to be improved. On the other hand, if it is preferable to increase resilience to milder windstorms, then the lines with the highest *RAW* values for $w_{\max} = 40$ m/s needs to be made more robust. It can also be seen that among the most critical lines are those supplying London (node 25), the largest demand node, e.g., circuits 34 and 45.

Further, Fig. 9(b) clearly indicates the criticality of each line and area based on the RAW_{EENS} analysis for $w_{\max} = 40$ m/s. As can be observed, the most critical areas of the test network for mitigating *EENS*, and thus increasing its resilience to weather-related power outages, mainly include the interconnections between North and South GB, as well as South GB where the large demand nodes are located.

D. Resilience Enhancement to Severe Wind Events

As aforementioned in Section III-B, the resilience enhancement case studies include "redundancy", "robustness" and "responsiveness" adaptation options. Fig. 1 shows the approach followed here for making the towers and lines more resistant to the wind event, represented by a translation of the fragility curves (indicated by "robust" in Fig. 1).

These case studies are applied on the transmission corridors according to their contribution to system resilience, as this is determined based on their RAW_{EENS} indices. In particular, a parallel, identical transmission corridor is added for the "redundant case", the resistance to high wind speeds of the transmission corridor is increased for the "robustness" case, and the time to repair of a transmission corridor is considered unaffected and equal to TTR_{normal} for the "responsiveness" case. However, instead of applying these resilience enhancement strategies to a single, individual line, e.g., between nodes 1 and 2, the transmission corridors are divided in resilience enhancement groups based on their RAW_{EENS} indices, with each group including 5 corridors (shown by dotted lines in Fig. 9). That is, the first group will include the first 5 most critical circuits of each wind level, the second group will include the first 10 critical circuits, the third group the first 15 critical circuits, and so on, up to the 50 circuits that are included in the test network. For example, for $w_{\max} = 60$ m/s, the first resilience enhancement group of circuits will include the ones with ID 45, 29, 41, 34 and 37 (which lines will be made more robust, more responsive and redundant), while the second group will include the ones with ID 45, 29, 41, 34, 37, 42, 44, 38, 18 and 19, and so on for the other groups. For $w_{\max} = 50$ m/s, the first resilience enhancement group of circuits will include the ones with ID 45, 34, 29,

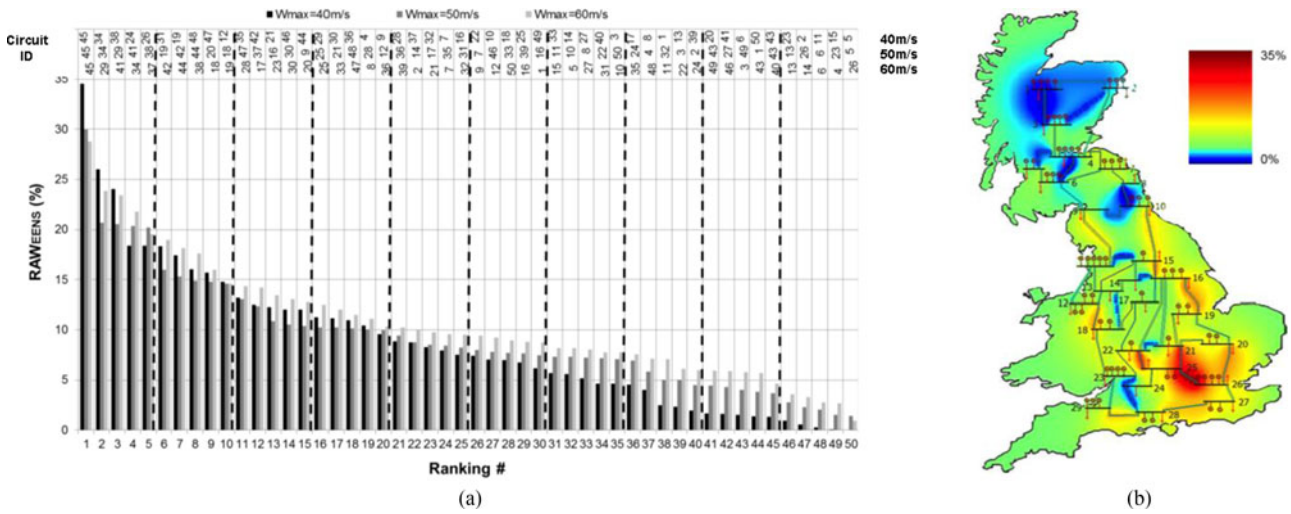

Fig. 9. Ranking of circuits based on their RAW_{EENS} indices per wind level (dotted lines indicate the groups of transmission circuits per wind level for which the resilience enhancement studies are subsequently applied). a) RAW_{EENS} ranking of transmission circuits. b) RAW_{EENS} mapping for $w_{\max} = 40$ m/s.

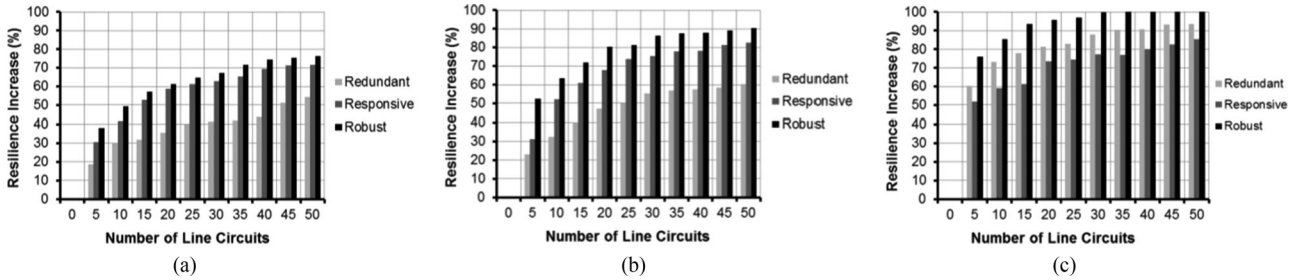

Fig. 10. Effect of resilience enhancement for different wind levels (base = no resilience enhancement). a) $w_{\max} = 60$ m/s. b) $w_{\max} = 50$ m/s. c) $w_{\max} = 40$ m/s.

41 and 38, while the second group will include the ones with ID 45, 34, 29, 41, 38, 19, 42, 44, 20 and 18, and so on.

Fig. 10 shows the percentage increase in the resilience by applying the resilience adaptation measures, as expressed using the decrease in *EENS* (similar results are obtained for *LOLF*). The horizontal axis of Fig. 10 shows the number of lines (or the number of resilience enhancement groups, e.g., 5 lines = 1 group, 10 lines = 2 groups, and so on) for which the case studies are applied. There is a big increase in resilience (i.e., drop in *EENS*) for the case studies when the first 5 critical lines are enhanced, e.g., close to 40% for the robust case for $w_{\max} = 60$ m/s. Resilience is further increased when the resilience of additional individual lines is improved, but this becomes smoother (especially for 50 m/s and 40 m/s), which is expected because as their RAW_{EENS} decreases, their contribution to the overall test network resilience decreases.

Comparing the effectiveness of the resilient measures, it can be seen that making the transmission lines and towers more robust to the wind event has the highest impact, i.e., higher increase in resilience, for all the wind levels. This is because it results in the lowest wind-affected failure probabilities of the components. It is also worth noting that for $w_{\max} = 40$ m/s the resilience increase reaches almost 100% in the robust case when about half of the circuits (i.e., 25–30 circuits) are made more robust. This type of technical insights can again be key to inform potential investment strategies.

It can also be observed that for $w_{\max} = 60$ m/s and 50 m/s the responsive case has a higher impact than the redundant, because the fast response to the numerous circuit outages due to the wind event is critical. However, making the components redundant becomes more effective (i.e., higher percentage increase in resilience) for $w_{\max} = 40$ m/s, where the components can withstand the wind event, leading to a much smaller number of wind-related outages. The fast response to the circuit outages thus becomes less important than having additional transmission assets. Again, this shows that depending on the targeted resilience event (in this case, $w_{\max}$), different mitigation options may be more or less adequate, with also different economic impact. Further, it is highlighted that the prioritization of resilience enhancement interventions might change for different wind speeds.

V. Conclusions

This paper has described and demonstrated a probabilistic methodology to assess and evaluate adaptation measures to

increase the resilience of power systems to extreme weather. An integral part of the proposed methodology is the consideration of the multi-temporal and multi-regional fragility of power system components to extreme weather conditions, with focus on the resistance of transmission network to extreme wind events. Further, differently from previous works, the resilience evaluation is performed using a mix of *infrastructure* and *operational* indices, allowing the systematic estimation of the resilience degradation of a transmission network subject to extreme weather and the development of strategies for boosting the key infrastructure and operational resilience features. The illustration of the proposed methodology using the reduced version of the GB transmission network clearly highlights its capability of assessing and quantifying the resilience of power systems to severe weather and the effect of different resilience enhancement strategies, based on the *RAW* index. Our results clearly demonstrate that the criticality of network sections depends on wind speed. Hence, as the projected changes to the wind environment resulting from climate change are highly uncertain, adaptation strategies need to be flexible.

The methodology presented in this paper is applicable to any power system and capable of modelling the effect of any weather event or natural disaster, as well as the combined impact of multiple weather parameters (e.g., wind and rain) on power systems resilience, as demonstrated in [18]. This can be done provided that the required information is available, which includes hazard characteristics, corresponding fragility models for these hazards, which can be provided through different ways, such as empirically, experimentally, analytically, etc., and the repair times for each component.

Future work will develop a cost/benefit analysis and a decision making framework for both operational and reinforcement measures to enable the determination of a practical and economical roadmap to transition power networks towards higher levels of resilience.

REFERENCES

[1] IPCC, "Climate change 2013: The physical science basis," *Contrib. Work. Group I 5th Assess. Rep. Intergovernmental Panel Climate Change*, 2013.

[2] P. SouthWell, "Disaster recovery within a cigre strategic framework: Network resilience, trends and areas of future work," *SC C1 CIGRE Tech. Committee*, Aug. 2014.

[3] R. Billinton and K. E. Bollinger, "Transmission system reliability evaluation using Markov processes," *IEEE Trans. Power App. Syst.*, vol. PAS-87, no. 2, pp. 538–547, Feb. 1968.

[4] Y. Liu and C. Singh, "Reliability evaluation of composite power systems using Markov cut-set method," *IEEE Trans. Power Syst.*, vol. 25, no. 2, pp. 777–785, May 2010.

[5] M. R. Bhuiyan and R. N. Allan, "Inclusion of weather effects in composite system reliability evaluation using sequential simulation," *Inst. Electr. Eng. Proc.-Gener., Transm. Distrib.*, vol. 141, no. 6, pp. 575–584, 1994.

[6] K. Alvehag and L. Soder, "A reliability model for distribution systems incorporating seasonal variations in severe weather," *IEEE Trans. Power Del.*, vol. 26, no. 2, pp. 910–919, Apr. 2011.

[7] L. Gengfeng *et al.*, "Risk analysis for distribution systems in the northeast U.S. under wind storms," *IEEE Trans. Power Syst.*, vol. 29, no. 2, pp. 889–898, Mar. 2014.

[8] M. Panteli and P. Mancarella, "Modeling and evaluating the resilience of critical electrical power infrastructure to extreme weather events," *IEEE Syst. J.*, to be published.

[9] M. Panteli and P. Mancarella, "Influence of extreme weather and climate change on the resilience of power systems: Impacts and possible mitigation strategies," *Elect. Power Syst. Res.*, vol. 127, pp. 259–270, 2015.

[10] M. Vaiman *et al.*, "Risk assessment of cascading outages: Methodologies and challenges," *IEEE Trans. Power Syst.*, vol. 27, no. 2, pp. 631–641, May 2012.

[11] W. Yuan, J. Wang, F. Qiu, C. Chen, C. Kang, and B. Zeng, "Robust optimization-based resilient distribution network planning against natural disasters," *IEEE Trans. Smart Grid*, vol. 7, no. 6, pp. 1–10, Nov. 2016.

[12] M. Ouyang, L. Dueñas-Osorio, and X. Min, "A three-stage resilience analysis framework for urban infrastructure systems," *Struct. Safety*, vols. 36–37, pp. 23–31, 2012.

[13] R. Francis and B. Bekera, "A metric and frameworks for resilience analysis of engineered and infrastructure systems," *Rel. Eng. Syst. Safety*, vol. 121, pp. 90–103, 2014.

[14] M. Ouyang and L. Dueñas-Osorio, "Time-dependent resilience assessment and improvement of urban infrastructure systems," *Chaos*, vol. 22, 2012, Art. no. 033122.

[15] M. Ouyang and L. Dueñas-Osorio, "Multi-dimensional hurricane resilience assessment of electric power systems," *Struct. Safety*, vol. 48, pp. 15–24, 2014.

[16] A. Kwasinski, "Quantitative model and metrics of electrical grids'resilience evaluated at a power distribution level," *Energies*, vol. 9, no. 2, 2016, Art. no. 93.

[17] M. Panteli, D. N. Trakas, P. Mancarella, and N. D. Hatziargyriou, "Boosting the power grid resilience to extreme weather events using defensive islanding," *IEEE Trans. Smart Grid*, vol. 7, no. 6, pp. 2913–2922, Nov. 2016.

[18] S. Espinoza, M. Panteli, P. Mancarella, and H. Rudnick, "Multi-phase assessment and adaptation of power systems resilience to natural hazards," *Elect. Power Syst. Res.*, vol. 136, pp. 352–361, 2016.

[19] Y. Wang, C. Chen, J. Wang, and R. Baldick, "Research on resilience of power systems under natural disasters—A review," *IEEE Trans. Power Syst.*, vol. 31, no. 2, pp. 1604–1613, Mar. 2015.

[20] M. Panteli and P. Mancarella, "The grid: Stronger, bigger or smarter?: Presenting a conceptual framework of power system resilience," *IEEE Power Energy Mag.*, vol. 13, no. 3, pp. 58–66, May/Jun. 2015.

[21] C. Pickering, S. Dunn, and D. S. Wilkinson, "Securing community resilience by modern infrastructure design," in *Proc. 4th Int. Conf. Comput. Methods Struct. Dyn. Earthquake Eng.*, 2013, pp. 1–9.

[22] Hazus, Federal Emergency Management Agency. [Online]. Available: https://www.fema.gov/hazus, Accessed in: Oct. 2016.

[23] Keeping the country running: Natural hazards and infrastructure, Cabinet Office, London, U.K., Oct. 2011.

[24] J. F. Espiritu, D. W. Coit, and U. Prakash, "Component criticality importance measures for the power industry," *Elect. Power Syst. Res.*, vol. 77, pp. 407–420, 2007.

[25] M. Kirsty and K. R. W. Bell, "Wind related faults on the GB transmission network," in *Proc. Int. Conf. Probabilistic Methods Appl. Power Syst.*, 2014, pp. 1–6.

[26] K. E. Lindsey, *Transmission Emergency Restoration Systems For Public Power*. Azusa, CA, USA: Lindsey Manufacturing, 2015.

[27] R. Dawson and J. Hall, "Adaptive importance sampling for risk analysis of complex infrastructure systems," *Proc. Roy. Soc. Amer.*, vol. 462, pp. 3343–3362, 2006.

[28] F. Casciati and L. Faravelli, *Fragility Analysis of Complex Structural Systems*. Taunton, U.K.: Research Studies Press, 1991.

[29] S. Dunn, C. Galasso, S. Wilkinson, L. Manning, and D. Alderson, "Development of empirical fragility curves for electrical supply systems subjected to wind hazard," in *Proc. 12th Int. Conf. Appl. Statist. Probab. Civil Eng.*, 2015, pp. 1–8.

[30] Applied Technology Council, "Seismic performance assesment of buildings volume 1—Methodology," Redwood, CA, USA, *ATC-58-175*, 2011.

[31] M. D. Miller and J. C. Wong, *Guidelines for electrical transmission line structural loading*, 3rd ed. Washington, DC, USA: Amer. Soc. Civil Eng., 2010.

[32] P. Vincent, C. Huet, M. Charbonneau, P. Guillbault, M. Lapointe, and D. Banville, "Testing and numerical simulation of overhead transmission lines dynamics under component failure conditions," in *Proc. 40th General Session of CIGRÉ*, 2004, Paper B2-308.

[33] J. M. Eidinger and L. Kempner Jr., "Reliability of transmission towers under extreme wind and ice loading," in *Proc. 44th CIGRÉ Paris Session*, 2012, pp. 1–12.

[34] M. Belivanis and K. Bell, "Representative GB network model: Notes," Univ. Strathclyde, Glasgow, U.K., 2011.

[35] MERRA Re-analysis. 2016. [Online]. Available: http://gmao.gsfc.nasa.gov/research/merra/
[36] UK Met Office, UK climate-extremes. 2016. [Online]. Available: http://www.metoffice.gov.uk/public/weather/climate-extremes/
[37] UK Met Office, Beaufort wind force scale. 2016. [Online]. Available: http://www.metoffice.gov.uk/guide/weather/marine/beaufort-scale

Mathaios Panteli (S'09–M'13) received the M.Eng. degree from Aristotle University of Thessaloniki, Thessaloniki, Greece, in 2009, and the Ph.D. degree in electrical power engineering from The University of Manchester (UoM), Manchester, U.K., in 2013, where he also was a Postdoctoral Research Associate for a few years. In September 2015, he joined the University of Cyprus as a Research Associate and the University of Nicosia, Cyprus, as an Adjunct Lecturer. He is currently a Lecturer in the Power and Energy Division at UoM. His main research interests include analysis and prevention of blackouts, high-impact low-probability events, and risk and resilience assessment of future power systems.

Cassadra Pickering received the M.Eng. degree from Newcastle University, Newcastle upon Tyne, U.K., in 2011. She is currently a Research Scholar at Newcastle University. Her research interest is focussed on developing analytical fragility functions for National Grid transmission towers.

Sean Wilkinson received the M.Eng. degree in civil engineering from the Queensland University of Technology, Australia, in 1991, and the Ph.D. degree in earthquake engineering from the Queensland University of Technology in 1997. He is currently a Senior Lecturer of structural engineering at Newcastle University, Newcastle upon Tyne, U.K. His research interest focuses on building community resilience to natural hazards by understanding how critical infrastructure responds in a disaster.

Richard Dawson received the M.Eng. degree in civil engineering from Bristol University, Bristol, U.K, in 1999 and the Ph.D. degree in performance-based management of complex infrastructure systems from the Bristol University in 2003. He is currently a Professor of earth systems engineering at Newcastle University, Newcastle upon Tyne, U.K., where one of his main research interests is the development of new approaches to analyze environmental risks to infrastructure systems and the built environment.

Pierluigi Mancarella (M'08–SM'14) received the M.Sc. and Ph.D. degrees in electrical energy systems from the Politecnico di Torino, Torino, Italy, in 2002 and 2006, respectively. He is currently a Professor of smart energy systems at The University of Manchester, Manchester, U.K., and the Chair Professor of electrical power systems at The University of Melbourne, Australia. His research interests include multienergy systems modeling, power system integration of low carbon technologies, network investment under uncertainty, and risk and resilience of smart grids. He is an Editor of the IEEE TRANSACTIONS ON SMART GRID, an Associate Editor of the IEEE SYSTEMS JOURNAL, and an IEEE PES Distinguished Lecturer.